



Visible-light-induced aerobic photocatalytic oxidation of aromatic alcohols to aldehydes over Ni-doped NH₂-MIL-125(Ti)



Yanghe Fu^{a,b}, Long Sun^a, Huan Yang^a, Lai Xu^a, Fumin Zhang^a, Weidong Zhu^{a,*}

^a Key Laboratory of the Ministry of Education for Advanced Catalysis Materials, Institute of Physical Chemistry, Zhejiang Normal University, Jinhua 321004, People's Republic of China

^b State Key Laboratory of Photocatalysis on Energy and Environment, Fuzhou University, Fuzhou 350002, People's Republic of China

ARTICLE INFO

Article history:

Received 2 May 2015

Received in revised form 3 January 2016

Accepted 16 January 2016

Available online 21 January 2016

Keywords:

Photocatalysis

Visible light

Metal-organic frameworks

Molecular oxygen

Selective alcohol oxidation

ABSTRACT

The Ni-doped NH₂-MIL-125(Ti) catalyst was developed for the photocatalytic aerobic oxidation of aromatic alcohols upon visible light irradiation. The results show that different aromatic alcohols can be effectively transformed to their corresponding aldehydes with almost absolute selectivity using O₂ as the oxidant over Ni-doped NH₂-MIL-125(Ti) upon visible light irradiation. Compared with the parent catalyst NH₂-MIL-125(Ti), Ni-doped NH₂-MIL-125(Ti) exhibits a significantly enhanced photocatalytic activity for the selective oxidation of aromatic alcohols. Preliminary studies indicate that the doping of Ni nanoparticles into NH₂-MIL-125(Ti) could improve the visible-light harvesting, charge-separation, and electron-transport of the resultant catalyst, leading to the enhanced photocatalytic activity. The current work provides some guidance in the development of MOF-based photocatalysts for organic syntheses.

© 2016 Elsevier B.V. All rights reserved.

1. Introduction

The selective oxidation of aromatic alcohols to their corresponding aldehydes is one of the most important functional group transformations in organic chemistry, since aldehydes and their derivatives are important building blocks for producing fine chemicals. Traditional oxidants, such as KMnO₄, CrO₃, Br₂, and TBHP (*tert*-butyl hydroperoxide), used in the oxidation process of aromatic alcohols, are usually toxic, corrosive or expensive [1–4]. On the contrary, the direct oxidation of aromatic alcohols to the aldehydes with molecular oxygen as oxidant can afford an economical and green way for this type of transformation. Furthermore, it would be ideal if this transformation can be realized by means of photocatalysis, since photocatalysis is considered to be a more economical and green process [5]. However, the strong oxidative potential of radicals and holes formed on the surface of photocatalysts in the UV-induced chemical reactions always promotes a complete mineralization, leading to unselective photocatalysis [6]. It is well known that TiO₂ has a strong oxidation ability and cannot make a full use of visible light due to a positive valence band of 2.7 eV and a wide energy gap of 3.2 eV [vs. normal hydrogen electrode (NHE) at pH 7]. It has been proven that TiO₂ can oxidize

all organics to CO₂, H₂O, and mineral acids, which cannot achieve the selective oxidation of alcohols to aldehydes using O₂ as oxidant under UV light [7]. To bypass these drawbacks, visible-light photocatalysis is favored in order to facilitate higher selectivities. Actually, visible-light induced photocatalysis is recently emerging as a promising strategy for the selective oxidation of aromatic alcohols using O₂ over modified TiO₂, CdS, In₂S₃, g-C₃N₄ and so on [8–11]. For example, Zhang et al. have investigated the aerobic oxidation of alcohols to the corresponding aldehydes with high selectivity using a special coupled system consisting of dye-sensitized TiO₂ and TEMPO (2,2,6,6-tetramethylpiperdinyloxy) upon visible light irradiation [8]. Although their work significantly improved the photocatalytic activity and selectivity for the aerobic oxidation of alcohols, a great effort should be still made on the development of efficient photocatalysts for industrial application.

Metal-organic frameworks (MOFs) are a class of crystalline micro-mesoporous hybrid materials that have already shown a variety of applications [12–18]. Their metal cluster building blocks, inherent large surface areas, uniform but tunable cavities, and tailorable chemistry make them to be promising catalysts or catalyst supports. Since the metal clusters in MOFs can be regarded as inorganic semiconductor quantum entities while the organic linkers as antenna activate these semiconductor quantum dots via the linker to metal cluster charge-transfer (LCCT) upon light excitation, it is believed that MOFs can also be promising photocatalysts [19]. The constitution and structure of MOFs are more flexible and tunable, as

* Corresponding author.

E-mail addresses: weidongzhu@zjnu.cn, wzhudelft@yahoo.com (W. Zhu).

compared with semiconductors, making MOFs extremely attractive as photocatalysts. In fact, recently, more and more photocatalysts based on MOFs applied in CO₂ reduction, hydrogen evolution, and organic syntheses have already been demonstrated [20–29]. Their performance can be enhanced by introduction of additional catalytic species, but these are commonly based on noble metals and the MOF typically only acts as container [30–33]. Inspired by natural photosynthesis, we envision a multi-component system that would allow for efficient photon capture, charge separation, electron transport, and catalytic turnover at different locations of a guest@MOF composite. This would offer an efficient charge transfer between a stable, photo-active MOF structure and doped species in the MOF upon visible light irradiation [34]. To achieve this overall modular design, the composite should contain redox-active (multi) metallic nodes such as Fe, Co, and Ni to allow charge separation and accumulation of electrons. To the best of our knowledge, the effects of the doping of transition metals, which are more attractive to practical applications, into MOFs on their photocatalysis have not been investigated yet.

In the current work, Ni-doped NH₂-MIL-125(Ti) catalysts are prepared and used as photocatalysts for the aerobic oxidation of aromatic alcohols to the corresponding aldehydes with O₂ as oxidant upon visible light irradiation. An attempt is to elucidate the effects of the doped Ni nanoparticles (NPs) on the photocatalysis.

2. Experimental

2.1. Materials

2-Aminoterephthalic acid (H₂ATA) was purchased from Alfa Aesar Co. Tetra-*n*-butyl titanate [Ti(OC₄H₉)₄] and nickel(II) chloride hexahydrate (NiCl₂·6H₂O) were purchased from Shanghai Chemical Reagent Co. Dry dimethylformamide (DMF) and methanol (MeOH) were purchased from Sigma Aldrich Co. Benzyl alcohol, *p*-methyl benzyl alcohol, *p*-methoxy benzyl alcohol, *p*-chloro benzyl alcohol, *p*-nitro benzyl alcohol, benzaldehyde, *p*-methyl benzaldehyde, *p*-methoxy benzaldehyde, *p*-chloro benzaldehyde, and *p*-nitro benzaldehyde were purchased from Aladdin Industrial Co. All reagents with AR purity (analytical reagent grade) were used as received without further purification.

2.2. Synthesis

2.2.1. NH₂-MIL-125(Ti)

H₂ATA (0.54 g, 3 mmol) and Ti(OC₄H₉)₄ (0.26 mL, 0.75 mmol) were added into a solution containing DMF (9 mL) and dry MeOH (1 mL) and stirred for 30 min at room temperature. The prepared solution was then transferred to a Teflon-lined stainless steel autoclave (50 mL) and the synthesis was carried out without agitation in an oven at 150 °C for 3 days. Once the synthesis was completed, the resultant suspension was filtered, washed with DMF and MeOH separately, extracted by Soxhlet extractor with MeOH, and finally dried to obtain a bright-yellow solid product.

2.2.2. Ni-doped NH₂-MIL-125(Ti)

The prepared NH₂-MIL-125(Ti) was heated to 120 °C for 3 h to remove the adsorbed molecules from the pores. The solution of MeOH (0.5 mL) with NiCl₂·6H₂O (40 mg) was added to the activated NH₂-MIL-125(Ti) (1.0 g) drop by drop. The mixture was stirred for 12 h at room temperature, then filtered and dried at 150 °C for 3 h. The resultant powder was reduced by an aqueous NaBH₄ solution (20 mL, 0.05 M), and thoroughly washed with deionized water. Lastly, the powder was dried under N₂ atmosphere at 60 °C for 10 h to obtain the Ni-doped NH₂-MIL-125(Ti) with a nominal Ni doping of 1.0 wt.%.

2.3. Characterization

The powdered X-ray diffraction (XRD) patterns were obtained on a Philips PW3040/60 diffractometer using Cu K α radiation (λ = 0.1541 nm) in a scanning range of 2–10° at 0.5°/min. The textural properties of the prepared samples were determined by N₂ adsorption/desorption at –196 °C using a Micromeritics ASAP 2020 instrument. The sample was outgassed in vacuum at 150 °C for 10 h prior to the adsorption measurement. The UV–vis diffuse reflectance spectroscopy (DRS) measurements were performed using a Shimadzu UV-3600 spectrophotometer equipped with an integrating sphere attachment, the analysis range was from 200 nm to 800 nm, and BaSO₄ was used as a reflectance standard. The scanning electron microscope (SEM) observations were performed on a Hitachi S-4800 apparatus equipped with a field emission gun. The transmission electron microscopy (TEM) observations were carried out on a JEOL JEM-1200 working at 200 kV. The sample was diluted in ethanol to give a 1:5 volume ratio and sonicated for 10 min. The ethanol slurry was then dropped onto a Cu grid covered with a thin film of carbon. The surface electronic states of the synthesized samples were investigated by X-ray photoelectron spectroscopy (XPS, Thermo Scientific EscaLab 250Xi using Al K α radiation). The XPS data were internally calibrated, fixing the binding energy of C 1s at 284.6 eV. After digestion of Ni-doped NH₂-MIL-101(Ti) (0.05 g) in a solution of 2 mL HF (40 wt.%) and 8 mL H₂SO₄ (98 wt.%) diluted to 100 mL with deionized water, the Ni loading of the prepared catalyst was determined by an IRIS Intrepid IIXSP inductively coupling plasma-atomic emission spectrometer (ICP-AES).

2.4. Electrochemistry measurements

The electrochemical analysis was carried out in a conventional three electrode cell, using two Pt plates as counter and reference electrodes, respectively. The working electrode was prepared on fluorine-doped tin oxide (FTO) glass, which was cleaned by sonication in deionized water and ethanol for 30 min, and then dried. The FTO slide was dip-coated with 10 mL of slurry, which was obtained from the mixture of 5 mg photocatalyst and 0.5 mL H₂O under sonication for 2 h, and the side part of the FTO slide was previously protected using Scotch tape. After air drying naturally, a copper wire was connected to the side part of the FTO glass using a conductive tape. The uncoated parts of the electrode were isolated with an epoxy resin, and the exposed area of the electrode was 0.25 cm². The working electrodes were immersed in a 0.2 M Na₂SO₄ aqueous solution without any additive for 30 s prior to the measurement. The photocurrent measurements were conducted with a CHI440A workstation (Shanghai Chenhua Instruments Co.). A 300 W Xe lamp (Beijing Perfectlight, PLS-SXE 300c) with a 420 nm cut-off filter was used as a light source.

2.5. Evaluation of photocatalytic activity

The photocatalytic oxidation of aromatic alcohols was carried out in a sealed reaction tube pre-saturated with O₂ atmosphere upon visible light irradiation at room temperature. The photocatalyst (50 mg) suspended in the solvent of benzotrifluoride (BTF) (6 mL) with aromatic alcohol (0.3 mmol) was degassed and saturated with O₂ before the photocatalytic reaction. The reaction was performed under the irradiation of a 300 W Xe lamp with a UV cut-off filter to remove all wavelengths less than 420 nm and an IR cut-off filter to remove all wavelengths larger than 800 nm. The reaction products were analyzed using a GC-FID (Agilent 6890A) with a HP-5 capillary column. The mass balance of aromatic alcohols and the produced aldehydes was >99% and no byproduct was detected.

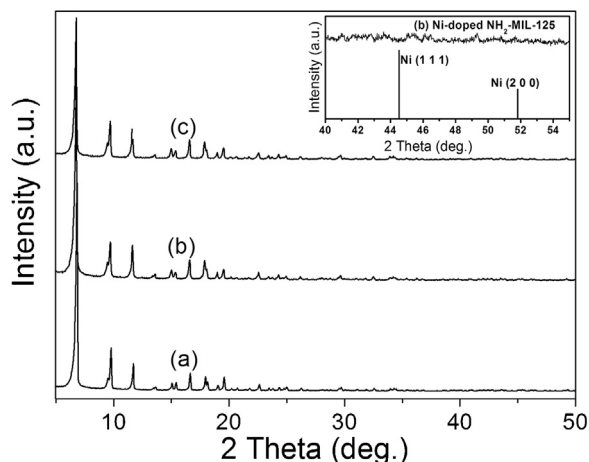


Fig. 1. XRD patterns of NH₂-MIL-125(Ti) (a), Ni-doped NH₂-MIL-125(Ti) (b), and the Ni-doped NH₂-MIL-125(Ti) after the 3rd-run reaction (c). The inset shows the XRD pattern of Ni.

3. Results and discussion

The Ni-doped NH₂-MIL-125(Ti) catalyst was synthesized by the wet-impregnation, followed by the reduction using the aqueous NaBH₄ solution. The doped amount of Ni into NH₂-MIL-125(Ti) is 0.93 wt.%, determined by the ICP-AES analysis, slightly lower than a nominal amount of 1 wt.%. The synthesized samples were characterized by means of various techniques. As shown in the XRD patterns in Fig. 1, the doping of Ni into NH₂-MIL-125(Ti) does not influence the crystallinity of NH₂-MIL-125(Ti) and no characteristic peak of Ni NPs is found due to the low loading and high dispersion of Ni on the MOF. The specific surface area of Ni-doped NH₂-MIL-125(Ti) is 993 m² g^{−1} with a pore volume of 0.59 cm³ g^{−1}, which is lower than that of NH₂-MIL-125(Ti) (1300 m² g^{−1} with a pore volume of 0.68 cm³ g^{−1}), which are derived from the adsorption isotherms of N₂ at −196 °C, shown in Fig. 2. The decrease in the surface area and pore volume of Ni-doped NH₂-MIL-125(Ti), in comparison with those of NH₂-MIL-125(Ti), may be ascribed to the

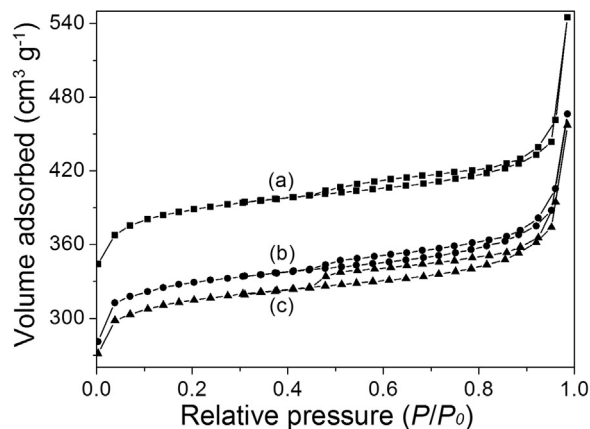


Fig. 2. N₂ adsorption/desorption isotherms of NH₂-MIL-125(Ti) (a), Ni-doped NH₂-MIL-125(Ti) (b), and the Ni-doped NH₂-MIL-125(Ti) after the 3rd-run reaction (c).

partial blocking of the cavities in NH₂-MIL-125(Ti) by the deposited Ni NPs. Fig. 3 displays the SEM and HR-TEM images of Ni-doped NH₂-MIL-125. It can be seen that Ni NPs immobilized into NH₂-MIL-125(Ti) have a mean diameter of 3 nm. The observed lattice spacings of 0.176 nm and 0.241 nm correspond to the (2 0 0) plane of cubic Ni (JCPDS, NO. 04-0850) and the (1 1 1) plane of NiO (JCPDS, NO. 47-1049), respectively, see Fig. 3c and d. In order to confirm the observation by HRTEM, the XPS technique was employed to investigate the valence states of Ni species in Ni-doped NH₂-MIL-125(Ti). Fig. 4 depicts the high-resolution XPS spectrum for the Ni NPs in Ni-doped NH₂-MIL-125, in which there are two peaks with Ni 2p_{3/2} binding energies of 852.7 and 855.2 eV, respectively, indicating the presence of the metallic and oxidative Ni in the nanoparticles [35]. The oxidized Ni may come from the partial oxidation during the preparation and washing processes. It is well known that Ni NPs are very active to be oxidized, and their activity tends to increase with declining their particle size. Once Ni NPs are separated from the reaction solution and exposed to atmosphere, they can be quickly oxidized [36].

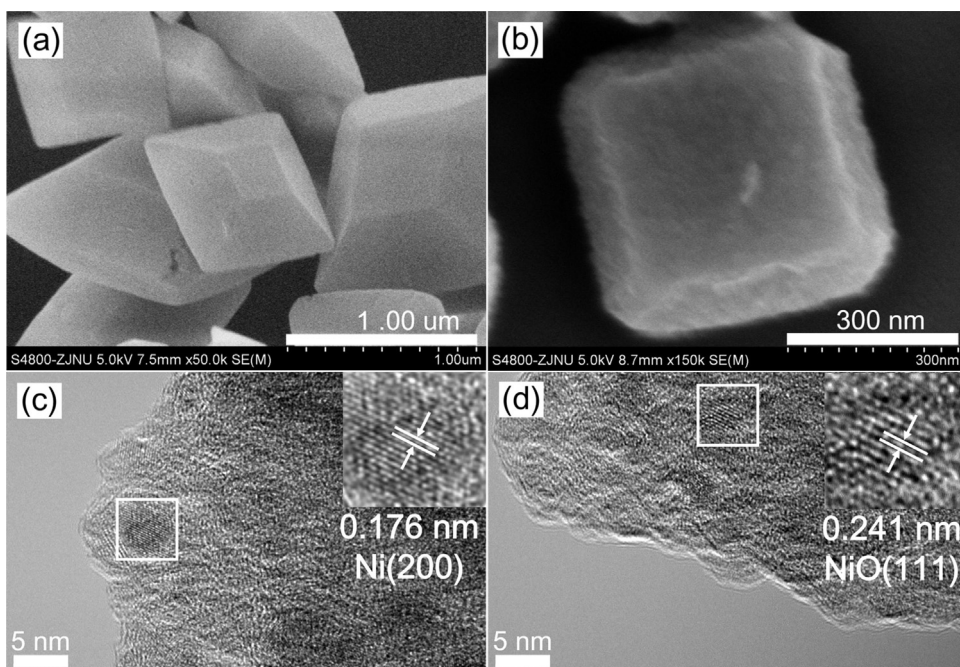


Fig. 3. SEM images (a and b) and HRTEM images (c and d) of Ni-doped NH₂-MIL-125(Ti).

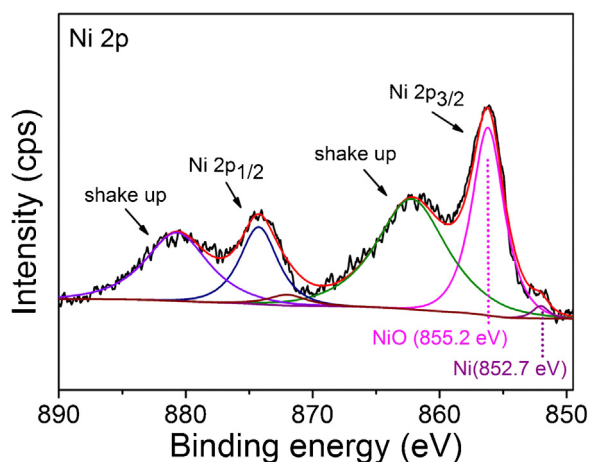


Fig. 4. High-resolution XPS spectra for Ni 2p of Ni-doped NH₂-MIL-125(Ti).

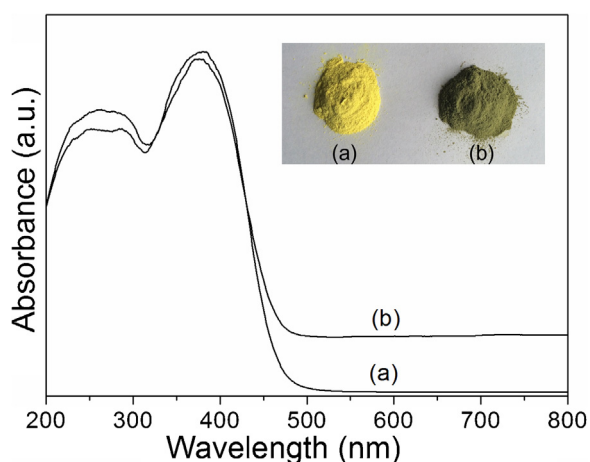


Fig. 5. UV-vis diffuse reflectance spectra of NH₂-MIL-125(Ti) (a) and Ni-doped NH₂-MIL-125(Ti) (b). The inset shows the colors of both samples.

A significant change in NH₂-MIL-125(Ti) immobilized with Ni NPs is of optical absorption characteristic. As shown in Fig. 5, NH₂-MIL-125(Ti) possesses two absorption edges extending to around 350 nm and 550 nm, corresponding to the absorption of Ti-O oxoclusters and the ligand-based absorption, respectively [20], while Ni-doped NH₂-MIL-125(Ti) has an extra absorption band in the visible light region of 500–800 nm, which is in accordance with the color change of the samples, from bright yellow [NH₂-MIL-125(Ti)] to dark green [Ni-doped NH₂-MIL-125(Ti)] (inset in Fig. 5). The enhanced absorbance of visible light is expected to improve the photocatalytic performance of Ni-doped NH₂-MIL-125(Ti) toward the target reactions.

The selective aerobic oxidation of *p*-methyl benzyl alcohol, a classic reaction, was employed to evaluate the photocatalytic properties of Ni-doped NH₂-MIL-125(Ti). The reaction was conducted using O₂ as the oxidant upon visible light irradiation, and the corresponding results were summarized in Table 1. In comparison with NH₂-MIL-125(Ti), a significant improvement in the catalytic activity is achieved by the Ni NPs deposited in NH₂-MIL-125(Ti), i.e., the conversion of *p*-methyl benzyl alcohol on NH₂-MIL-125(Ti) is only 25.8% while the conversion on Ni-doped NH₂-MIL-125(Ti) is enhanced to 43.2%, see entries 1 and 2 in Table 1. The controlled experiments were also conducted in the absence of visible light (entry 3) or without catalyst but upon visible light irradiation (entry 4) for 10 h. The results show that *p*-methyl benzyl alcohol is hardly oxidized in the absence of visible light or without catalyst but upon

Table 1

Aerobic photocatalytic oxidation of *p*-methyl benzyl alcohol in the presence of different catalysts^a.

<chem>Cc1ccc(CCO)cc1.O=Cc1ccc(C)cc1</chem> $\xrightarrow[\text{Visible light, 10 h}]{\text{Catalyst, O}_2}$			
Entry	Catalyst	Conversion (%)	Selectivity (%)
1	NH ₂ -MIL-125(Ti)	25.8	>99
2	Ni-doped NH ₂ -MIL-125(Ti)	43.2	>99
3 ^b	Ni-doped NH ₂ -MIL-125(Ti)	–	–
4 ^c	–	–	–
5	NiCl ₂ ·6H ₂ O	–	–
6 ^d	NiCl ₂ ·6H ₂ O + NH ₂ -MIL-125(Ti)	25.1	>99
7 ^e	NiO + NH ₂ -MIL-125(Ti)	26.0	>99
8 ^f	Ni-doped NH ₂ -MIL-125(Ti)	43.4	>99

^a Reaction conditions unless otherwise specified: 50 mg of catalyst and 0.3 mmol of *p*-methyl benzyl alcohol in 6 ml of BTF at room temperature for 10 h.

^b In dark.

^c Without photocatalyst but upon visible light irradiation.

^d With NiCl₂·6H₂O (0.5 mg) and NH₂-MIL-125(Ti) (45 mg).

^e With NiO (0.5 mg) and NH₂-MIL-125(Ti) (45 mg).

^f Reaction for 4 h after the photocatalyst was filtrated at the reaction of 10 h.

visible light irradiation. In addition, there is no any conversion of *p*-methyl benzyl alcohol in the presence of Ni²⁺ in the reaction mixture (entry 5) and the conversions over NH₂-MIL-125(Ti) in the presence of Ni²⁺ (entries 6 and 7) are almost the same as that over only NH₂-MIL-125(Ti) (entry 1), implying that the enhanced activity of Ni-doped NH₂-MIL-125(Ti) results from the metallic Ni but not from the nickel(II) salt and/or the oxidized Ni species. The use of solid catalyst can make the workup procedure very simple: the catalyst can easily be recovered after the reaction by filtration and can be reused without significant loss of catalytic activity or selectivity. However, leaching and/or deactivation of heterogeneous catalysts are often responsible for severe drawbacks and are frequently observed. To further verify whether Ni-doped NH₂-MIL-125(Ti) is truly heterogeneous or not, the catalyst was removed from the reaction medium by filtration after 10 h of reaction and the experiment proceeded with the filtrate under the same conditions (entry 8). The reaction was completely stopped by the removal of Ni-doped NH₂-MIL-125(Ti), verifying that the catalytic reaction was truly heterogeneous and occurred over the solid catalyst rather than in the solution.

In order to demonstrate the reusability of Ni-doped NH₂-MIL-125(Ti), a three-cycle experiment was performed, and the results are shown in Fig. 6. Clearly, the conversions of *p*-methyl benzyl alcohol and the selectivities for the desired product are almost the same in the three runs in succession, verifying the reusability of Ni-doped NH₂-MIL-125(Ti). Additionally, the results from the N₂-adsorption/desorption and XRD characterizations for the used Ni-doped NH₂-MIL-125(Ti) catalyst after the 3rd-run reaction are almost identical to those for the fresh one, as shown in Figs. 1 and 2, further confirming the stability of Ni-doped NH₂-MIL-125(Ti).

The substrate scope of the aerobic oxidation of aromatic alcohols over Ni-doped NH₂-MIL-125(Ti) was also investigated, and these results are summarized in Table 2. Remarkably, the aromatic alcohols are converted into the corresponding aldehydes with high selectivity (>99%) in all the cases. Similarly, compared with NH₂-MIL-125(Ti), Ni-doped NH₂-MIL-125(Ti) shows an enhanced activity for the selective oxidation of the aromatic alcohols. In addition, it appears that the substituents' electronics have a significant impact on the conversions (10.5–47.4%) over Ni-doped NH₂-MIL-125(Ti). In comparison with bare benzyl alcohol, the alcohols with electron withdrawing substituents on the phenyl ring exhibit the decreased conversions (10.5–20.6%) while those bearing electron donating ones show the enhanced conversions (43.2–47.4%).

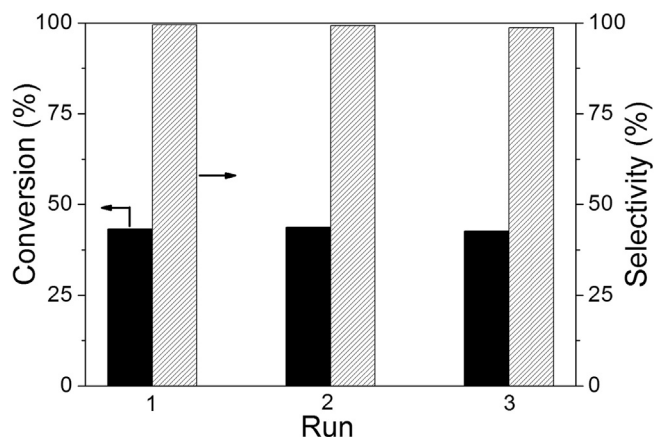


Fig. 6. Reusability of Ni-doped NH₂-MIL-125(Ti) in the aerobic oxidation of *p*-methyl benzyl alcohol upon visible light irradiation. Reaction conditions: 50 mg of catalyst and 0.3 mmol of *p*-methyl benzyl alcohol in 6 ml of BTF at room temperature for 10 h.

Table 2

Aerobic photocatalytic oxidation of aromatic alcohols over NH₂-MIL-125(Ti) and Ni-doped NH₂-MIL-125(Ti) upon visible light irradiation^a.

Entry	-R	Conversion (%)		Selectivity (%)
		NH ₂ -MIL-125(Ti)	Ni-doped NH ₂ -MIL-125(Ti)	
1	-NO ₂	8.2	10.5	>99
2	-Cl	11.8	20.6	>99
3	-H	12.5	21.5	>99
4	-CH ₃	25.8	43.2	>99
5	-OCH ₃	42.5	47.4	>99

^a Reaction conditions: 50 mg of catalyst and 0.3 mmol of aromatic alcohol in 6 ml of BTF at room temperature for 10 h.

The photocatalytic reduction of CO₂ over NH₂-MIL-125(Ti) revealed that an electron transferred from the excited ligand to the Ti-O oxo-clusters (LMCT) to form Ti³⁺ under visible light is responsible for CO₂ reduction to form HCOO⁻ [20]. Similarly, it is proposed that Ti³⁺ is also involved in the aerobic oxidation of the alcohols to the corresponding aldehydes over Ni-doped NH₂-MIL-125(Ti). Upon visible light irradiation, the excited ligand H₂ATA can transfer an electron to Ti-O oxo-clusters to form Ti³⁺ moiety. The as-formed Ti³⁺ can react with molecular oxygen to generate •O₂⁻ while Ti³⁺ is oxidized back to Ti⁴⁺. In the meantime, the alcohols can donate electrons, followed by a de-protonation process to generate the aldehydes. In fact, the use of alcohols as electron donors has been reported [20,37]. When the Ni NPs are introduced into NH₂-MIL-125(Ti), visible-light harvesting will be more efficient and the electron from the alcohols can be rapidly transferred to the excited H₂ATA. Moreover, the synergistic effect of Ni and Ti species may be responsible for the higher photocatalytic activity for the selective oxidation of the alcohols, attributed to the higher efficiency in charge formation and separation, based on metal-to-metal charge-transfer excitation [38,39]. The photo-generated charge separation efficiency of the Ni-doped sample is further confirmed by the transient photocurrent density response in an on-off cycle mode, as shown in Fig. 7. Upon visible light irradiation, in comparison with NH₂-MIL-125(Ti), Ni-doped NH₂-MIL-125(Ti) shows the enhancement of the long-term steady photocurrent density response by ca. three times. It is believed that the stronger photocurrent intensity can be attributed to the higher photocatalytic performance because of the more efficient charge separation. Consequently, it can be

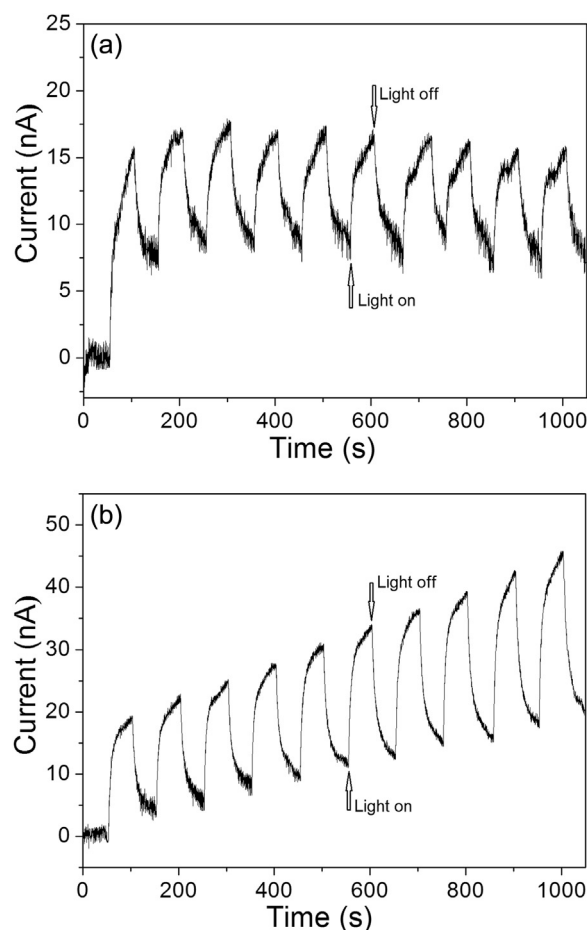


Fig. 7. Transient photocurrent responses of NH₂-MIL-125(Ti) (a) and Ni-doped NH₂-MIL-125(Ti) (b) in 0.2 M Na₂SO₄ aqueous solution without bias versus Ag/AgCl upon visible light irradiation ($\lambda \geq 420$ nm).

inferred that the doping of Ni NPs into NH₂-MIL-125(Ti) could facilitate the visible-light harvesting and photo-induced charge transfer.

4. Conclusions

The selective photocatalytic oxidation of several alcohols to their corresponding aldehydes using O₂ as oxidant can be achieved over Ni-doped NH₂-MIL-125(Ti) upon visible light irradiation. Therefore, the current work provides some guidance in the development of photocatalysts for an economical, sustainable and thus green process for the transformation of alcohols, which is of utmost importance in the chemical industry. Compared with NH₂-MIL-125(Ti), Ni-doped NH₂-MIL-125(Ti) shows an enhanced photocatalytic activity for the selective oxidation, probably ascribed to the more efficient visible-light harvesting and effective electron transfer by the doping of Ni NPs into NH₂-MIL-125(Ti). Although the performance of Ni-doped NH₂-MIL-125(Ti) on the selective oxidation of the alcohols should be improved to a great extent for industrial application, the current study also highlights the great potential of MOF-based photocatalysts for organic synthesis.

Acknowledgements

We are grateful for the financial support by the National Natural Science Foundation of China (21303166 and 21476214).

References

- [1] J. Lou, M. Wang, L.-Y. Zhu, Z. Fang, *Catal. Commun.* 4 (2003) 647–649.
- [2] M.E. González-Núñez, R. Mello, A. Olmos, R. Acerete, G. Asensio, *J. Org. Chem.* 71 (2006) 1039–1042.
- [3] R. Liu, X. Liang, C. Dong, X. Hu, *J. Am. Chem. Soc.* 126 (2004) 4112–4113.
- [4] G.C. Behera, K.M. Parida, *Appl. Catal. A-Gen.* 413–414 (2012) 245–253.
- [5] X. Lang, X. Chen, J. Zhao, *Chem. Soc. Rev.* 43 (2014) 473–486.
- [6] L. Zhang, D. Liu, J. Guan, X. Chen, X. Guo, F. Zhao, T. Hou, X. Mu, *Mater. Res. Bull.* 59 (2014) 84–92.
- [7] X. Lang, W. Ma, C. Chen, H. Ji, J. Zhao, *Acc. Chem. Res.* 47 (2014) 355–363.
- [8] M. Zhang, C. Chen, W. Ma, J. Zhao, *Angew. Chem. Int. Ed.* 47 (2008) 9730–9733.
- [9] N. Zhang, Y. Zhang, X. Pan, X. Fu, S. Liu, Y.-J. Xu, *J. Phys. Chem. C* 115 (2011) 23501–23511.
- [10] M. Xie, X. Dai, S. Meng, X. Fu, S. Chen, *Chem. Eng. J.* 245 (2014) 107–116.
- [11] F. Su, S. Mathew, C.G. Lipner, X. Fu, M. Antonietti, S. Blechert, X. Wang, *J. Am. Chem. Soc.* 132 (2010) 16299–16301.
- [12] A. Corma, H. García, F.X.L. Xamena, *Chem. Rev.* 110 (2010) 4606–4655.
- [13] J.-R. Li, J. Sculley, H.-C. Zhou, *Chem. Rev.* 112 (2012) 869–932.
- [14] T.R. Cook, Y.-R. Zheng, P.J. Stang, *Chem. Rev.* 113 (2013) 734–777.
- [15] P. Horcjada, R. Gref, T. Baati, P.K. Allan, G. Maurin, P. Couvreur, G. Férey, R.E. Morris, C. Serre, *Chem. Rev.* 112 (2012) 1232–1268.
- [16] L.J. Murray, M. Dincă, J.R. Long, *Chem. Soc. Rev.* 38 (2009) 1294–1314.
- [17] L. Ma, C. Abney, W. Lin, *Chem. Soc. Rev.* 38 (2009) 1248–1256.
- [18] G. Férey, *Chem. Soc. Rev.* 37 (2008) 191–214.
- [19] T. Tachikawa, J.R. Choi, M. Fujitsuka, T. Majima, *J. Phys. Chem. C* 112 (2008) 14090–14101.
- [20] Y. Fu, D. Sun, Y. Chen, R. Huang, Z. Ding, X. Fu, Z. Li, *Angew. Chem. Int. Ed.* 51 (2012) 3364–3367.
- [21] D. Sun, Y. Fu, W. Liu, L. Ye, D. Wang, L. Yang, X. Fu, Z. Li, *Chem. Eur. J.* 19 (2013) 14279–14285.
- [22] C.G. Silva, I. Luz, F.X.L. Xamena, A. Corma, H. García, *Chem. Eur. J.* 16 (2010) 11133–11138.
- [23] J. Long, S. Wang, Z. Ding, S. Wang, Y. Zhou, L. Huang, X. Wang, *Chem. Commun.* 48 (2012) 11656–11658.
- [24] M.A. Nasalevich, M.G. Goesten, T.J. Savenije, F. Kapteijn, J. Gascon, *Chem. Commun.* 49 (2013) 10575–10577.
- [25] D. Sun, L. Ye, Z. Li, *Appl. Catal. B: Environ.* 164 (2015) 428–432.
- [26] D. Wang, R. Huang, W. Liu, D. Sun, Z. Li, *ACS Catal.* 4 (2014) 4254–4260.
- [27] D. Wang, Z. Li, *Catal. Sci. Technol.* 5 (2015) 1623–1628.
- [28] D. Sun, W. Liu, M. Qiu, Y. Zhang, Z. Li, *Chem. Commun.* 51 (2015) 2056–2059.
- [29] Y. Lee, S. Kim, J.K. Kang, S.M. Cohen, *Chem. Commun.* 51 (2015) 5735–5738.
- [30] C. Wang, K.E. de Krafft, W. Lin, *J. Am. Chem. Soc.* 134 (2012) 7211–7214.
- [31] Y. Horiuchi, T. Toyao, M. Saito, K. Mochizuki, M. Iwata, H. Higashimura, M. Anpo, M. Matsuoka, *J. Phys. Chem. C* 116 (2012) 20848–20853.
- [32] D. Sun, W. Liu, Y. Fu, Z. Fang, F. Sun, X. Fu, Y. Zhang, Z. Li, *Chem. Eur. J.* 20 (2014) 4780–4788.
- [33] J. Canivet, S. Aguado, Y. Schuurman, D. Farrusseng, *J. Am. Chem. Soc.* 135 (2013) 4195–4198.
- [34] M.A. Nasalevich, R. Becker, E.V. Ramos-Fernandez, S. Castellanos, S.L. Veber, M.V. Fedin, F. Kapteijn, J.N.H. Reek, J.I. van der Vlugt, J. Gascon, *Energy Environ. Sci.* 8 (2015) 364–375.
- [35] P. Girault, J. Grosseau-Poussard, J. Dinhut, L. Marechal, *Nucl. Instrum. Methods B* 174 (2001) 439–452.
- [36] X. Li, H. Wang, T. Chu, D. Li, L. Mao, *Mater. Res. Bull.* 57 (2014) 254–259.
- [37] M. Dan-Hardi, C. Serre, T.O. Frot, L. Rozes, G. Maurin, C.M. Sanchez, G. Férey, *J. Am. Chem. Soc.* 131 (2009) 10857–10859.
- [38] S. Shen, J. Chen, R.T. Koodali, Y. Hu, Q. Xiao, J. Zhou, X. Wang, L. Guo, *Appl. Catal. B-Environ.* 150–151 (2014) 138–146.
- [39] L. Fan, J. Long, Q. Gu, H. Huang, H. Lin, X. Wang, *J. Catal.* 320 (2014) 147–159.